Geophysical Research Letters

Supporting Information for

The 2021 South Sandwich Island M_w 8.2 earthquake: a slow event sandwiched between regular ruptures

Zhe Jia[1*], Zhongwen Zhan[1], Hiroo Kanamori[1]

[1] Seismological Laboratory, California Institute of Technology, Pasadena, CA 91125, USA.

Contents of this file

Texts S1-S2
Figures S1 to S10
Table S1-S2

Introduction

This supporting information provides: two additional texts for the methods (Text S1-S2), 10 figures (Figure S1-S10), and two tables (Table S1-S2) to support the main text.

Text S1. W-phase inversion.

NEIC PDE listed 2 events:

8/12/2021 18:32:52 (UTC), depth=47.2 km, M_w=7.5

8/12/2021 18:35:17 (UTC), depth=22.8 km, M_w=8.1

These 2 events are only 145 s apart, and the standard W phase inversion for the 1st event could not converge at any reasonable solution because the W phases from the 2 events interfered. The standard inversion for the 2nd event did not work either for the same reason. For the 2nd event, only after several trials using different frequency bands, we could achieve a reasonable waveform fit with a relatively narrow low-frequency band 0.00125 to 0.002 Hz (*i.e.*, 500 to 800 s). This solution (Fig. S2) can fit the W phase waveforms reasonably well for 45 phases at 40 stations (Fig. S2). However, because of the very narrow band and the complex interference of phases, the centroid location, especially the depth, is poorly constrained (Fig. S3). The overall mechanism and size of the event seem to be reasonably well constrained. The centroid time shift, t_c, is 20 s from 18:35:17(UTC) which means that the centroid time of this event is 18:35:37(UTC) which is 165 s after the origin time of the 1st event. Thus we consider that this event approximately corresponds to the GCMT event 202108121832A (referred to as GCMT1, centroid time 18:35:25 UTC, M_w=8.3). However, the quality of the solution is not up to the standard W phase solution because of the complex waveform interferences of the multiple events of the sequence.

Text S2. Subevent inversion for the M_w 8.2 South Sandwich Island sequence.

We applied our subevent inversion method to simultaneously estimate the source parameters of 5 subevents. Each subevent has 10 point-source parameters, including 3 parameters for the subevent horizontal location and depth, a centroid time, a source time duration, and 5 deviatoric moment tensor elements. For the long-period subevent E3, we added two finiteness parameters, rupture velocity and rupture direction, to accommodate a Haskell unilateral rupture source with a constant rupture velocity. In this Haskell model, the dependence of the apparent source duration on rupture direction can be given by the following equation (local rise time is ignored),

$$D = D_0 \cdot \left(1 - \frac{V_r}{c} \cdot \cos(\theta - \varphi)\right)$$

, where D is the apparent source duration for a station of azimuth φ, D_0 is the rupture duration, V_r is the rupture velocity, c is the phase velocity, and θ is the rupture direction. In this study, we calculate phase velocities for teleseismic P and SH waves with ray tracing, using the IASPEI91 model. Because the regional full waveforms are dominated by surface waves, we assume c to be 4 km/s as approximate Rayleigh and Love phase velocities at a dominant period of 50s and 300s. Overall, this hybrid parameterization of point source and Haskell subevents has 52 unknown parameters.

To improve the searching efficiency, we divide our inversion procedure into two stages, where we search a part of these parameters nonlinearly and invert the data for other parameters in a linear way. The outer stage has a Markov Chain Monte Carlo (MCMC) inversion sampler that searches nonlinear parameters (subevent locations, centroid times, source durations, rupture velocity and rupture direction). Its random walk process to propose new models is driven by a Metropolis-Hasting algorithm. In each step, the model is proposed by perturbing one of the nonlinear parameters while keeping the other nonlinear parameter at their current values. Selection of the parameter being perturbed is random. This approach ensures a high acceptance rate and improves the efficiency of converging to an optimum, which, if given broad model space being searched and high quality data fitting, should be close to the global optima. For each set of nonlinear parameters, we can linearly invert the data for the moment tensors of subevents as the inner stage, because the observed time series can be linearly related by subevent moment tensors and their Green's functions when subevent locations and timing are available. In practice, we predict apparent source time functions at all stations using the subevent locations and timings, then convolve them with the corresponding Green's functions, and eventually invert for deviatoric subevent moment tensors by extending the linear framework to multiple sources. In this way, only 27 nonlinear parameters are searched through the MCMC inversion, and it's much easier to extensively explore the model space.

We generated 72 Markov Chains and eventually kept 24 of them to avoid being trapped in local minima. The initial sample for each chain is randomly generated from bounded uniform distributions. Our MCMC inversion incorporates a Bayesian framework that propagates the data error and prior knowledge to the model error. We set the prior of all unknown parameters to be uniform distributions. We also empirically set the data error to be 10% to accommodate the inaccurate assumptions of the wave propagation processes, even though the true data error (noise and instrumental error) of the seismic waves are very small. This data error eventually turns to the width of the Markov Chain sample distributions, which reflects the marginal posterior probability density functions.

We used 58 vertical component teleseismic (epicentral distance of 30°-90°) P waves in both displacement and velocity, 43 transverse component teleseismic SH waves in displacement, 12 three-component regional (epicentral distance within 40°) full waveforms in displacement in our subevent inversion from the Global Seismic Network and the International Federation of Digital Seismograph Networks. The weighting of these three datasets is set to be 20:10:1 to scale the teleseismic waves up for similar final misfit contributions. For the inversion of teleseismic waves, we calculate the Green's functions with a hybrid method that combines propagator matrix and ray theory, and use a combination of the CRUST2.0 velocity model at the source location with an IASPEI91 model in the deeper earth. A limitation of this forward simulation method is that it does not consider PP or SS phases, but since the M_w 7.5 foreshock is much smaller than the M_w 8.1 mainshock, the PP and SS amplitudes of the foreshock do not overwhelm the P and S of the mainshock, the waveform interferences are limited. We also compute the regional full waveform synthetics with a frequency-wavenumber integration algorithm using the PREM model as an average structure from sea to land. We used the P and S arrival times predicted from ray tracing with the IASPEI91 model, and allowed maximum time shifts of 4s, 6s and 10s for the P, SH, and regional full waves. Because all subevents could move their horizontal locations together with the seismograms shifting simultaneously, we need to fix the horizontal location of one subevent. Therefore, we anchored the location of the first subevent E1 at the hypocenter of the M_w 7.5 foreshock, assuming the rupture dimension between the initiation and centroid of E1 is small compared with the full sequence.

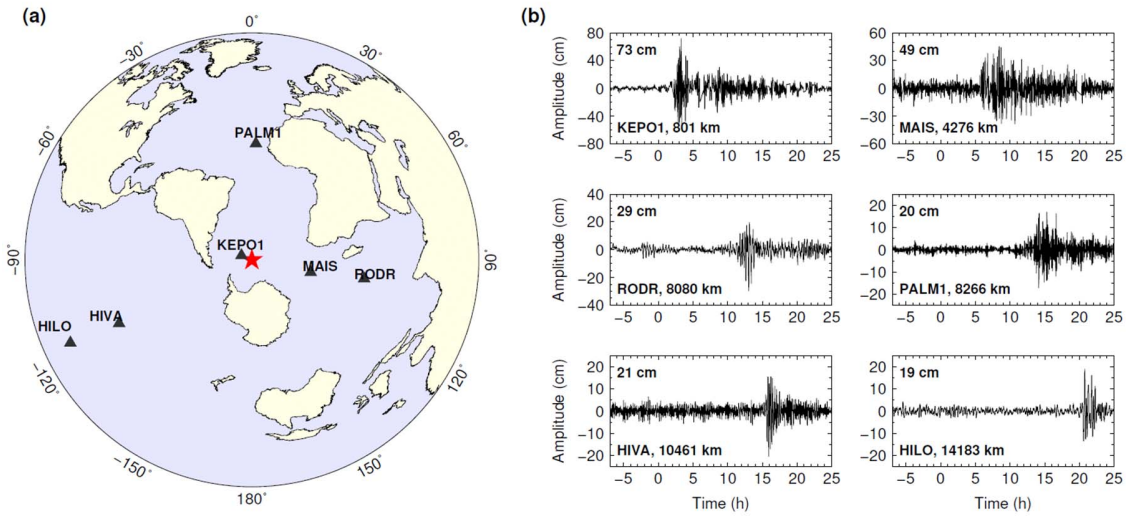
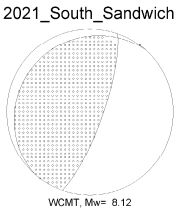


Figure S1. Tsunami of the South Sandwich Island sequence observed by tide gauges. (a) Distributions of the tide gauge stations (black triangles). The red star indicates the hypocenter of the South Sandwich Island sequence. (b) Waveforms recorded at the tide gauges in (a). The waveforms are high-pass filtered to periods shorter than 5 hours. The number above each trace shows the peak absolute amplitude of the tsunami. Below each trace the tide gauge station name and the distance from the South Sandwich Island earthquake source are shown.

(a)



Moment Tensor [dyn-cm x 1e28]: 0.8130 -0.2078 -0.6052 0.5270 1.6134 -0.3721
Scalar moment [dyn-cm]: 1.89e+28
Best Nodal planes (strike/dip/rake): NP1 221.8/ 13.7/ 111.8 NP2: 19.4/ 77.3/ 84.8
Eigenvalues (dyn-cm x 1e28): 1.8945 -0.0185 -1.8760 (Mw = 8.12)
Fit Quality: RMS: 0.00343 mm (0.417) GAP: 93.9°, C# 724
Filter parameters: filt_order: 4 filt_cf1 : 0.00125 filt_cf2 : 0.00200 filt_pass : 1

(b)

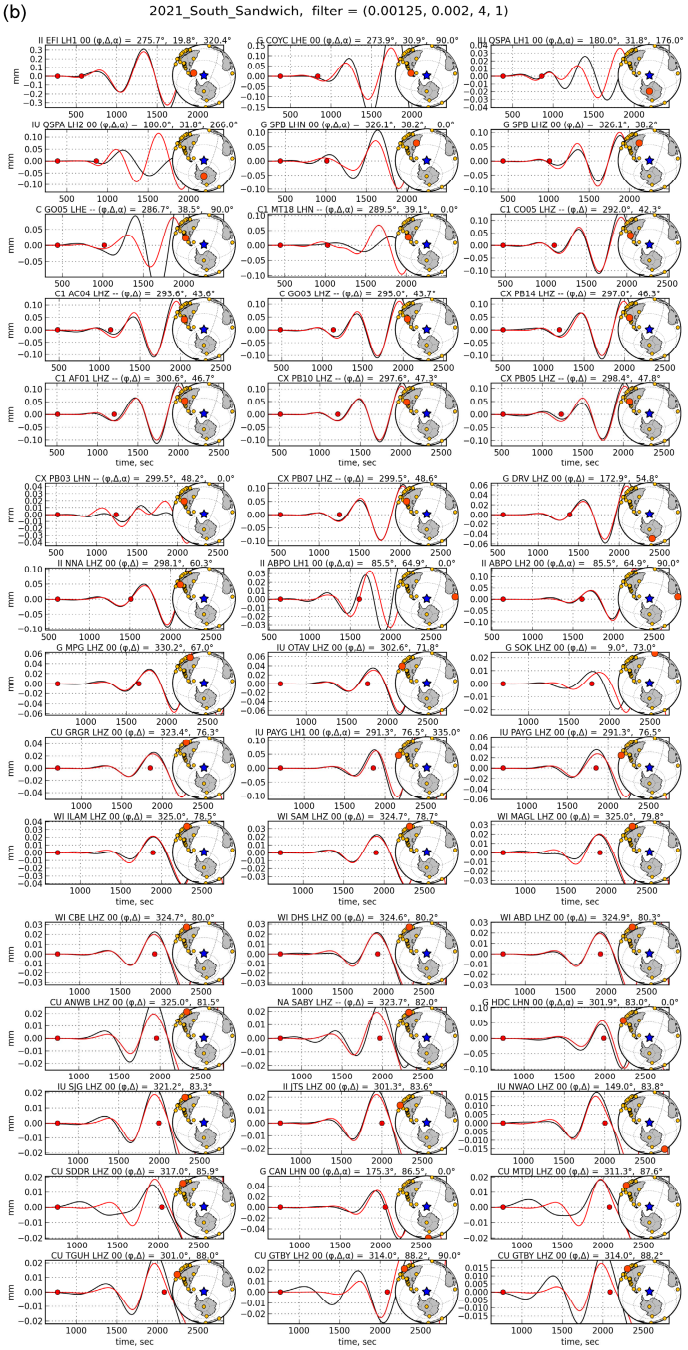


Figure S2. Long period W-phase point source solution for the 2021 South Sandwich Island sequence. (a) W-phase moment tensor and source parameters. The beachball shows the deviatoric moment tensor. The following lines display the moment tensor elements, scalar moment, and eigenvalues. The centroid depth is 30.5 km. (b) W-phase waveforms (between the red dots) for observation (black) and synthetics (red). Location of each station is indicated by the big red dot among the total set of stations used.

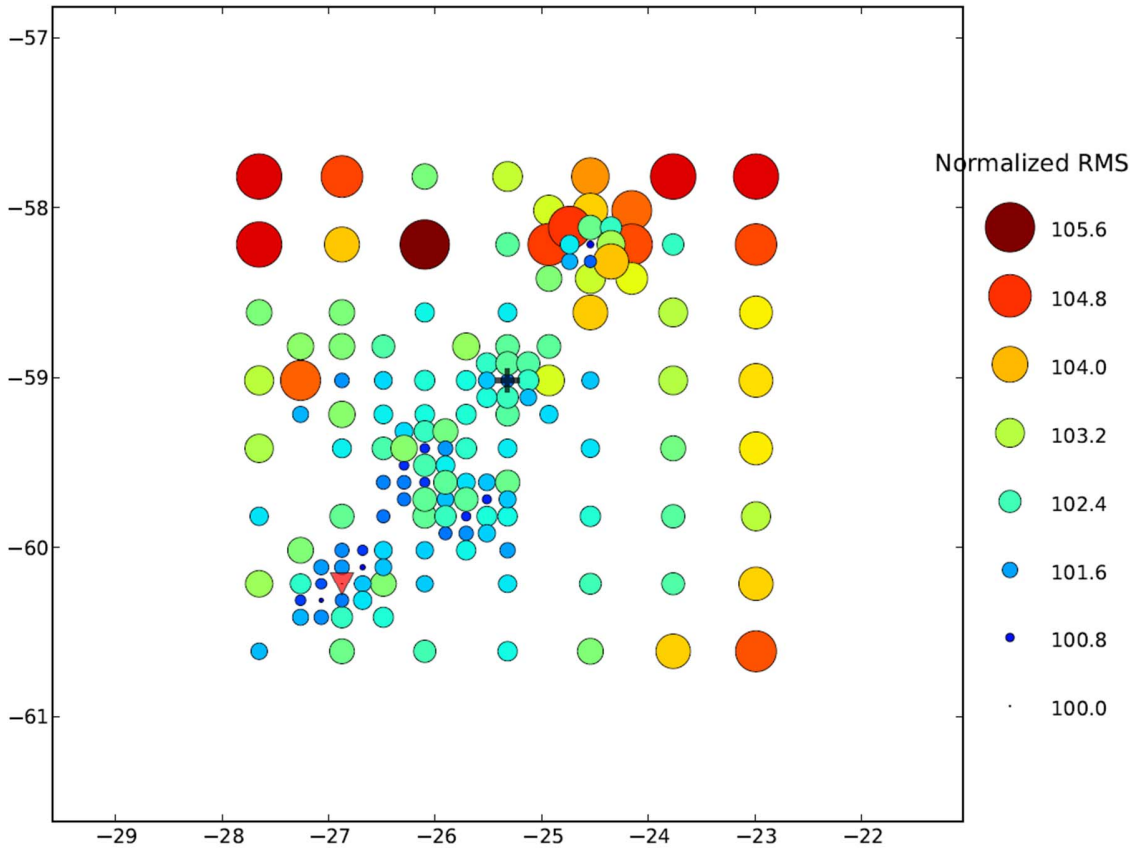


Figure S3. Resolution of location for the W-phase inversion. Circles indicate the searched locations. Their sizes and colors show the normalized root mean square misfit.

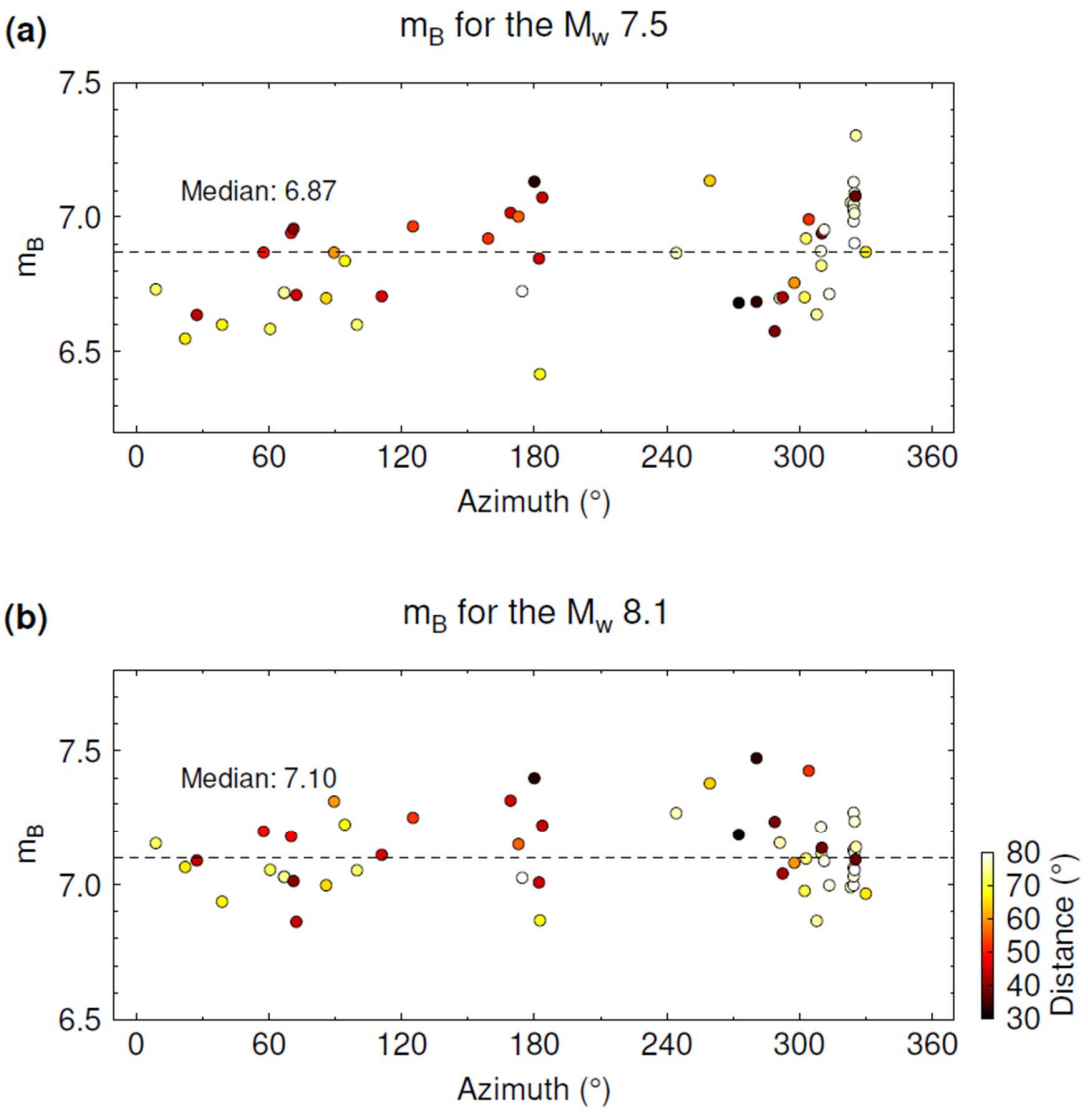


Figure S4. Body wave magnitudes of the South Sandwich Island sequence. (a) Individual body wave magnitudes m_B using stations at different azimuths (colored circles) for the M_w 7.5 foreshock. Colors show the epicentral distances. The black dashed line shows the median m_B of 6.87. (b) Same as (a), but for the M_w 8.1 mainshock. The median m_B is 7.10.

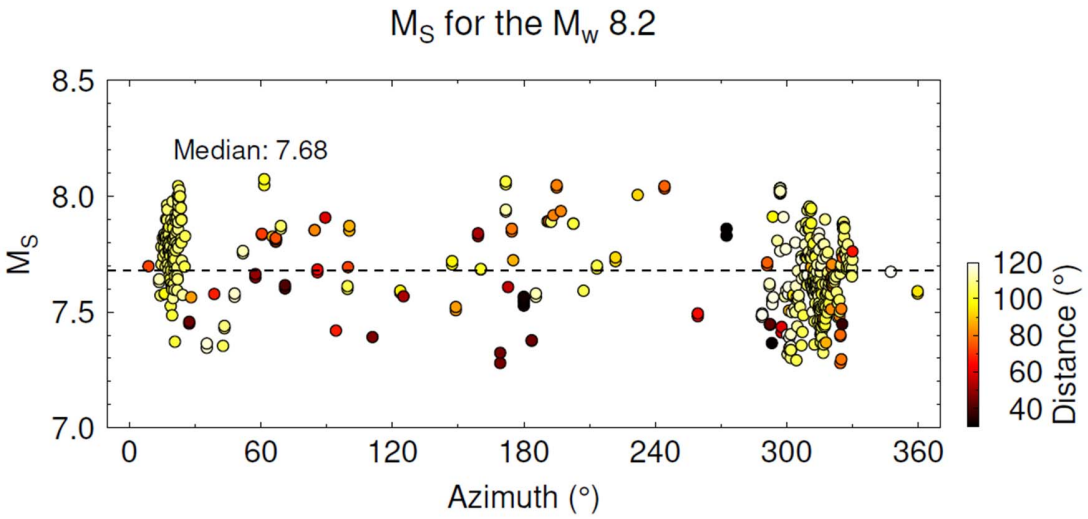


Figure S5. Surface wave magnitudes of the South Sandwich Island sequence. (a) Individual surface wave magnitudes M_S using stations at different azimuths (colored circles) for the overall M_w 8.2 South Sandwich Island sequence. Colors show the epicentral distances. The black dashed line shows the median m_S of 7.68.

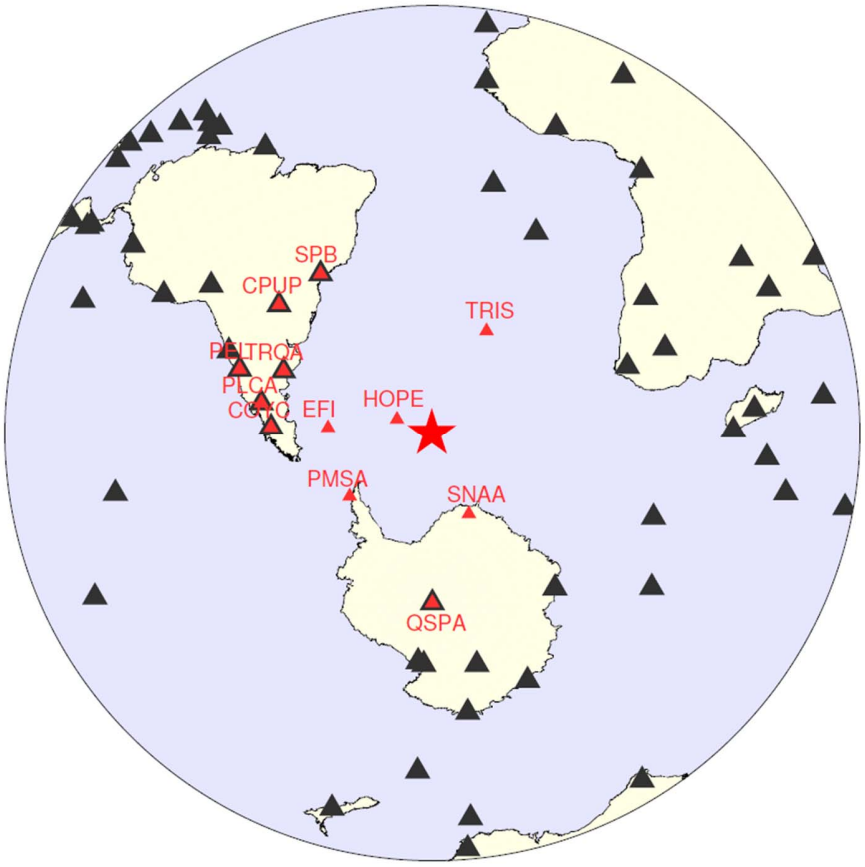


Figure S6. Seismic stations used in the subevent inversion. The red star shows the hypocenter of the South Sandwich Island sequence. Black and red triangles indicate the teleseismic (epicentral distance between 30° and 90°) and regional (epicentral distance within 40°) stations. Note that 7 of them are used for both teleseismic and regional inversions.

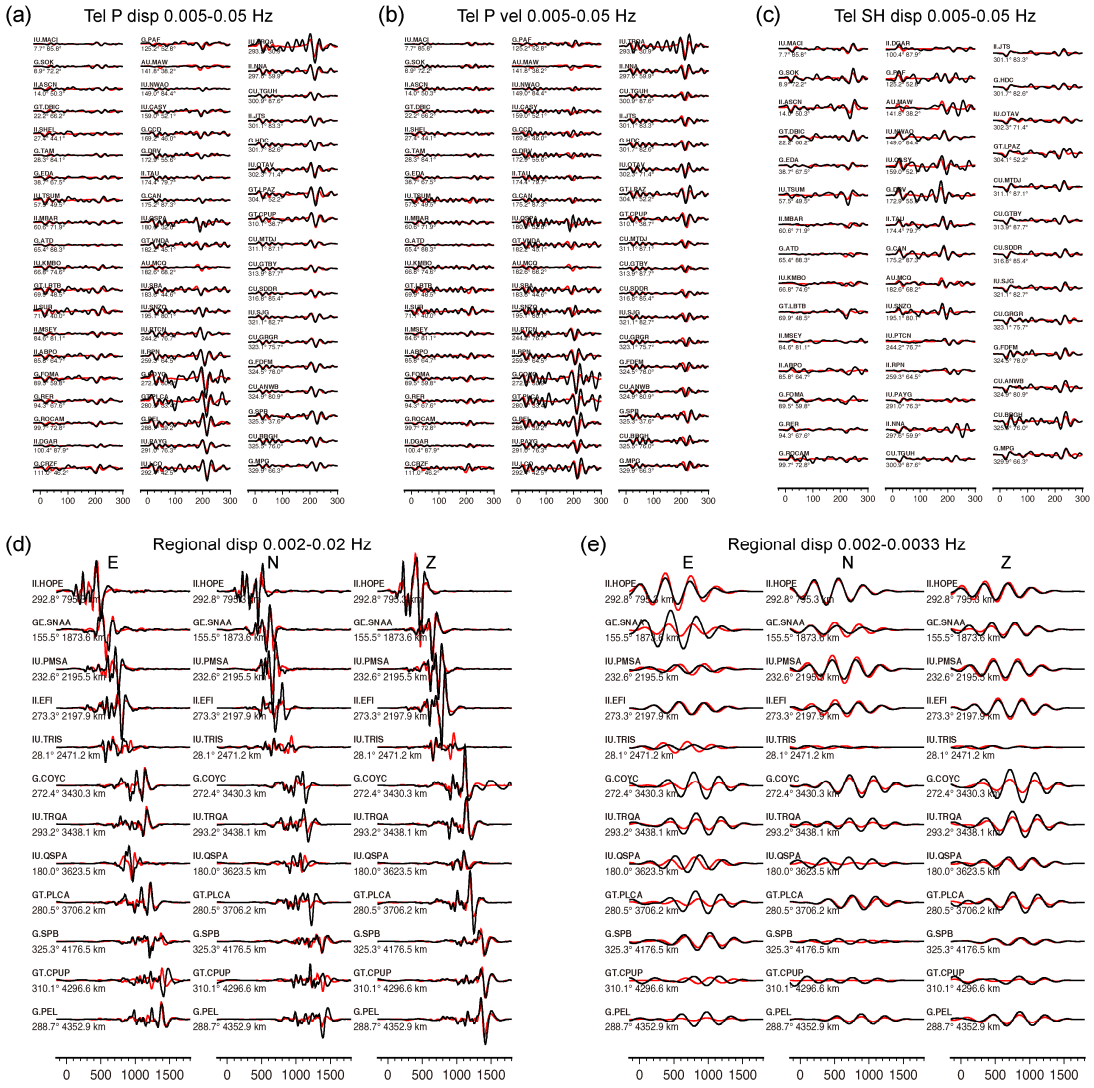


Figure S7. Waveform fits of the preferred subevent model for the South Sandwich Island sequence. Observed data and synthetics are indicated by black and red lines, respectively. The numbers leading each trace are the station azimuth and distance. (a) P waves in displacement. (b) P waves in velocity. (c) SH waves in displacement. (d) Intermediate period (0.002-0.02 Hz) regional full waveforms in displacement. (e) Long period (0.002-0.0033 Hz) regional full waveforms in displacement.

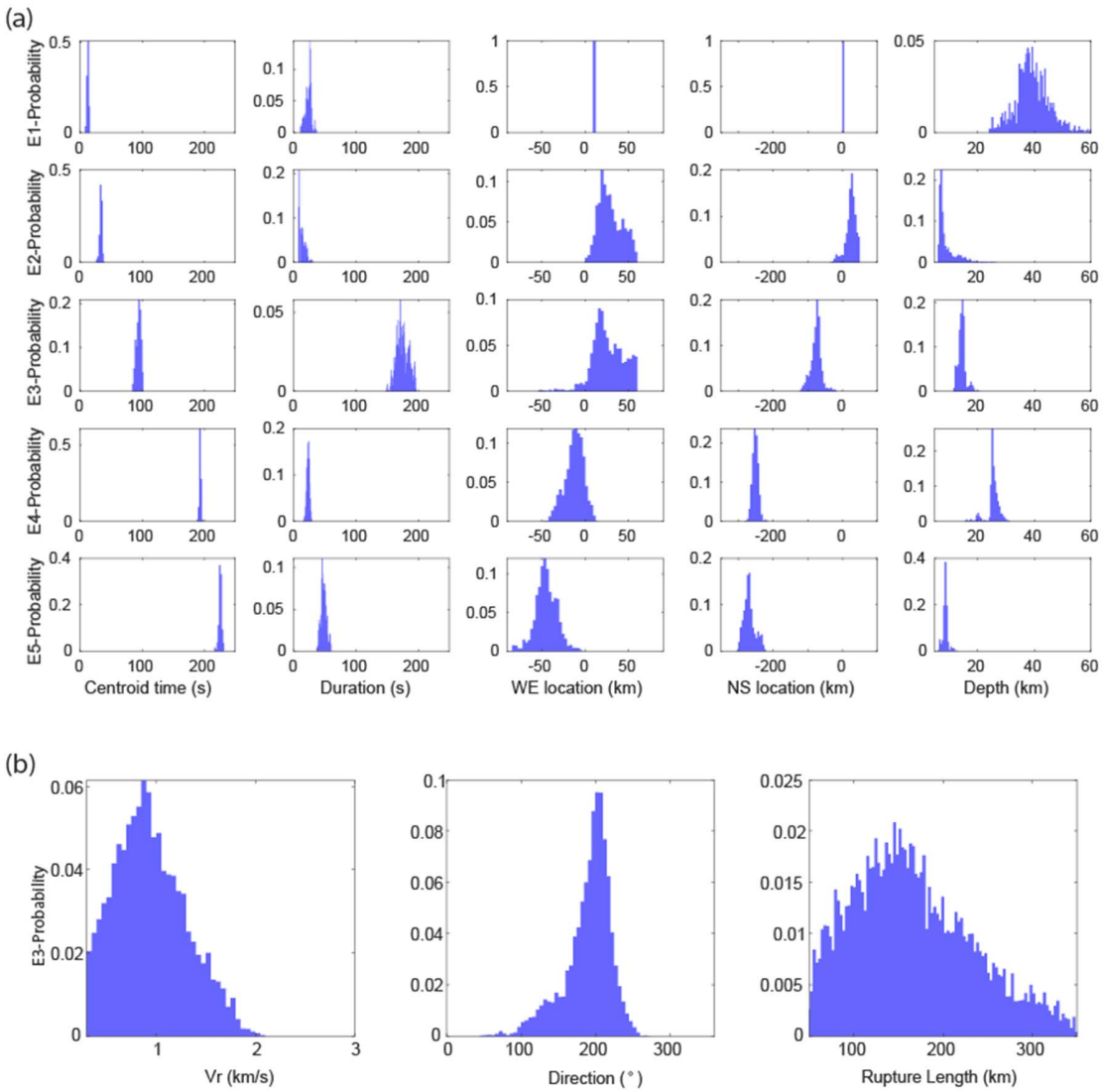


Figure S8. Assessment of subevent model uncertainties with the Markov Chain sample distributions. (a) Markov Chain sample distributions of the point source parameters. Columns from left to right indicate the marginal probability density distribution of subevent centroid times, durations, west-east locations, north-south locations and centroid depths. Rows represent subevents E1-E5. (b) Markov Chain sample distributions of finiteness parameters for the subevent E3. Columns are the rupture velocity, rupture direction (in degrees clockwise from the north), and rupture length.

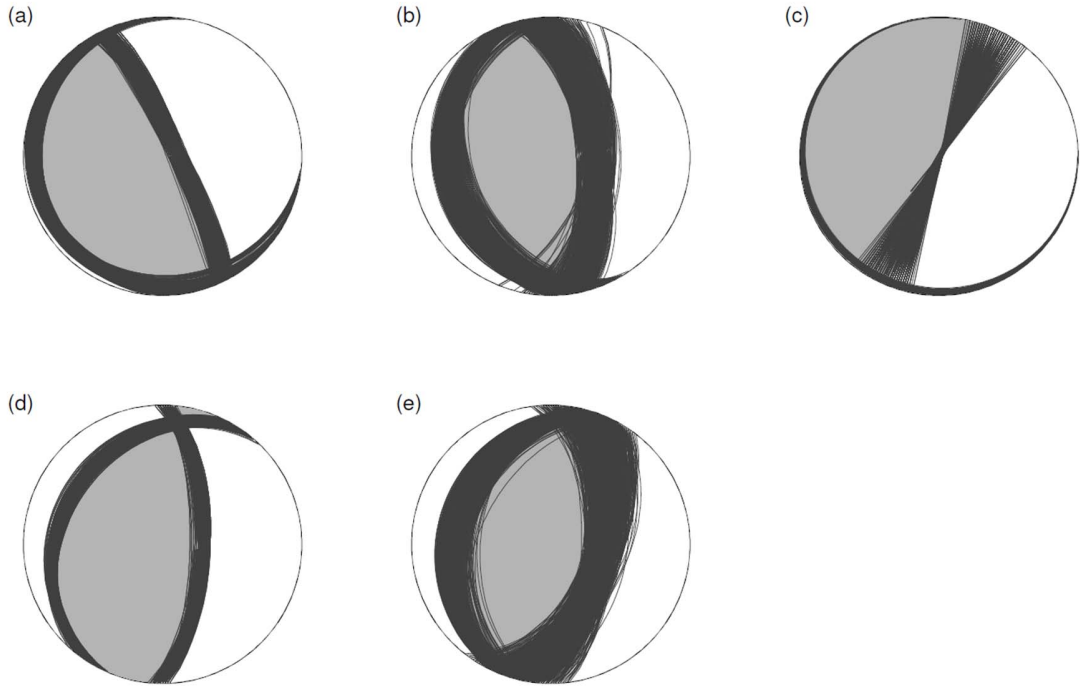


Figure S9. Ranges of double couple focal mechanisms for subevent E1 (a), E2 (b), E3 (c), E4 (d) and E5 (e) of the South Sandwich Island sequence.

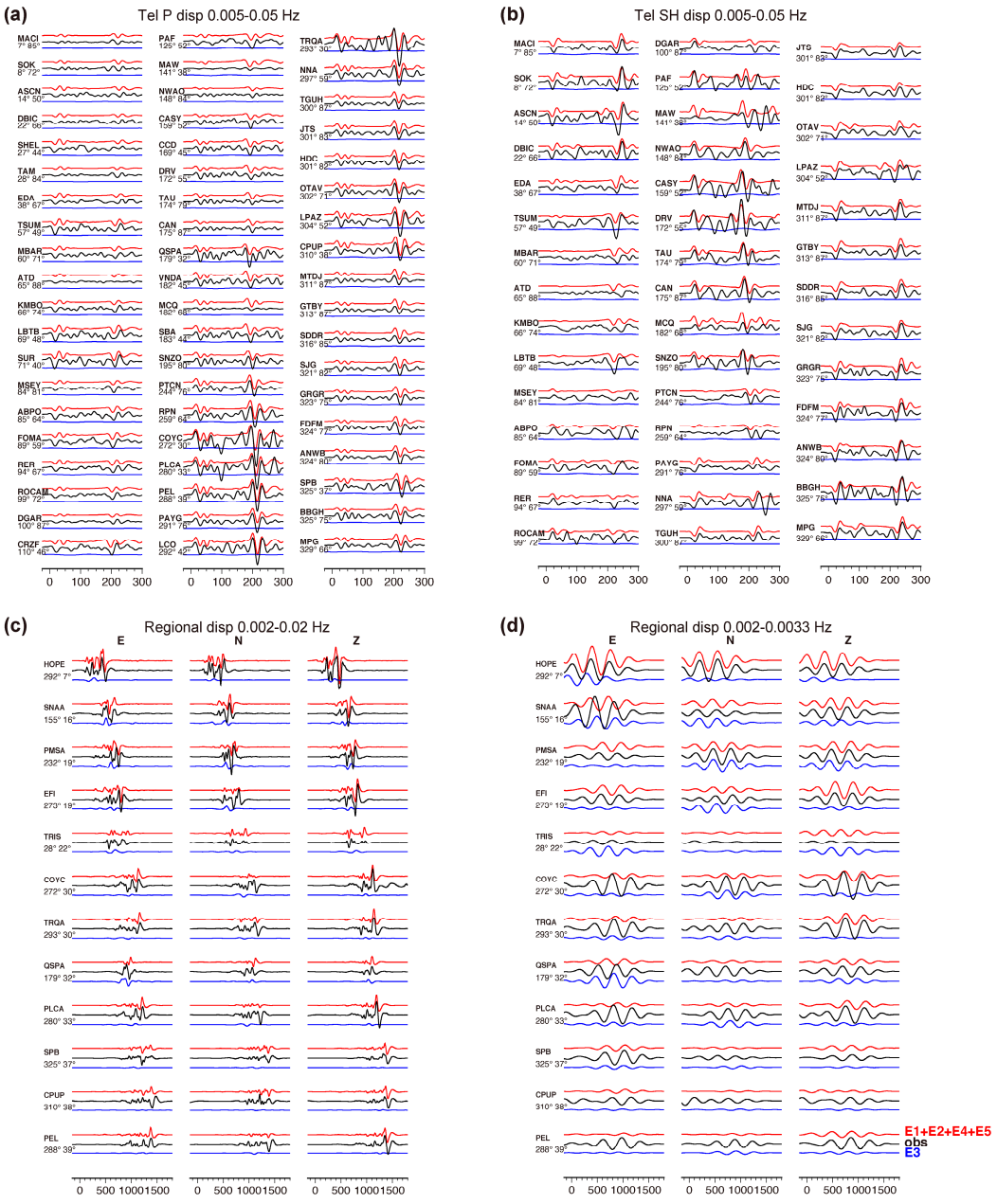


Figure S10. Contributions to waveforms from different groups of subevents. Black lines show the observed seismograms. Red lines represent the total contributions from regular subevents E1, E2, E4 and E5. Blue lines indicate the contribution from the slow subevent E3. Numbers leading traces are the station azimuths and distances. (a) P waves in displacement. (b) SH waves in displacement. (c) Intermediate period (0.002-0.02 Hz) regional full waveforms in displacement. (d) Long period (0.002-0.0033 Hz) regional full waveforms in displacement.

	Initiation time (UTC)	Centroid time (UTC)	Longitude (°)	Latitude (°)	Depth (km)	Magnitude	Strike (°)	Dip (°)	Rake (°)
NEIC1	18:32:52	NaN	-25.03	-57.68	47.2	7.5	NaN	NaN	NaN
NEIC2	18:35:17	NaN	-25.26	-58.38	22.8	8.1	NaN	NaN	NaN
GCMT1	NaN	18:35:25	-24.34	-59.48	20.0	8.3	204	14	118
GCMT2	NaN	18:36:13	-25.15	-60.47	15.1	7.9	195	22	64
USGSMwc	NaN	18:35:58	-24.90	-60.38	10.0	7.98	248	27	151
USGSMww	NaN	18:36:56	-23.16	-60.80	35.5	8.13	223	11	110
W-phase	NaN	18:35:33	-26.88	-60.22	30.5	8.12	222	14	112

Table 1. Source parameters for the South Sandwich Island earthquake from different catalogs.

	Centroid time (s)	Duration (s)	Longitude (°)	Latitude (°)	Rupture Velocity (km/s)	Rupture direction (°)	Depth (km)	Mrr (10^{20} N-m)	Mtt (10^{20} N-m)	Mpp (10^{20} N-m)	Mrt (10^{20} N-m)	Mrp (10^{20} N-m)	Mtp (10^{20} N-m)
E1	13.08	22.74	-25.03	-57.57	NaN	NaN	39.38	0.314	-0.104	-0.211	-0.301	0.669	0.083
E2	35.72	19.37	-24.82	-57.34	NaN	NaN	7.09	0.747	-0.151	-0.595	0.018	0.551	0.095
E3	90.38	176.12	-24.72	-58.28	1.01	187.06	14.26	2.469	-1.547	-0.922	8.191	19.743	2.049
E4	195.01	26.33	-25.64	-59.86	NaN	NaN	25.28	2.153	-0.304	-1.849	-0.236	2.268	-0.622
E5	226.37	50.40	-25.86	-60.00	NaN	NaN	8.94	3.315	-0.940	-2.375	0.704	2.917	-0.512

	Mo (10^{20} N-m)	M_w	Strike (°)	Dip (°)	Rake (°)
E1	0.79	7.20	150	11	84
E2	0.88	7.23	164	26	79
E3	21.58	8.16	134	4	22
E4	3.11	7.59	213	24	118
E5	4.25	7.69	199	22	94

Table 2. Subevent model parameters for the South Sandwich Island earthquake.